Molecular Vision 2015; 21:1328-1339 <http://www.molvis.org/molvis/v21/1328>
Received 23 July 2015 | Accepted 27 December 2015 | Published 29 December 2015

Mesenchymal–epithelial cell interactions and proteoglycan matrix composition in the presumptive stem cell niche of the rabbit corneal limbus

Keiko Yamada,[1,2] Robert D. Young,[1] Philip N. Lewis,[1] Katsuhiko Shinomiya,[2] Keith M. Meek,[1] Shigeru Kinoshita,[2] Bruce Caterson,[3] Andrew J. Quantock[1]

[1]Structural Biophysics Research Group, School of Optometry & Vision Sciences, Cardiff University, Maindy Road, Cardiff, UK; [2]Department of Ophthalmology, Kyoto Prefectural University of Medicine, 465 Kajii-cho, Kamigyo-ku, Kyoto-shi, Kyoto, Japan; [3]Connective Tissue Biology Laboratories, School of Biosciences, The Sir Martin Evans Building, Cardiff University, Museum Avenue, Cardiff, UK

Purpose: To investigate whether mesenchymal–epithelial cell interactions, similar to those described in the limbal stem cell niche in transplant-expired human eye bank corneas, exist in freshly enucleated rabbit eyes and to identify matrix molecules in the anterior limbal stroma that might have the potential to help maintain the stem cell niche.
Methods: Fresh limbal corneal tissue from adult Japanese white rabbits was obtained and examined in semithin resin sections with light microscopy, in ultrathin sections with transmission electron microscopy, and in three-dimensional (3D) reconstructions from data sets of up to 1,000 serial images from serial block face scanning electron microscopy. Immunofluorescence microscopy with five monoclonal antibodies was used to detect specific sulfation motifs on chondroitin sulfate glycosaminoglycans, previously identified in association with progenitor cells and their matrix in cartilage tissue.
Results: In the rabbit limbal cornea, while no palisades of Vogt were present, the basal epithelial cells stained differentially with Toluidine blue, and extended lobed protrusions proximally into the stoma, which were associated with interruptions of the basal lamina. Elongate processes of the mesenchymal cells in the superficial vascularized stroma formed direct contact with the basal lamina and basal epithelial cells. From a panel of antibodies that recognize native, sulfated chondroitin sulfate structures, one (6-C-3) gave a positive signal restricted to the region of the mesenchymal–epithelial cell associations.
Conclusions: This study showed interactions between basal epithelial cells and subjacent mesenchymal cells in the rabbit corneal limbus, similar to those that have been observed in the human stem cell niche. A native sulfation epitope in chondroitin sulfate glycosaminoglycans exhibits a distribution specific to the connective tissue matrix of this putative stem/progenitor cell niche.

The corneal limbus, as a transitional zone between the cornea and sclera, has long been a region of intense scientific interest with important functional roles in nutrient supply to the cornea and in the outflow of aqueous humor. However, in recent years, attention has focused on another essential function of the limbus, namely, as the site supporting corneal epithelial and mesenchymal stem cell populations that have the respective capability of renewing corneal epithelial cells and keratocytes, during normal homeostasis and in wound healing [1-4].

Studies of corneal epithelial stem cells far exceed in number those dedicated to stromal and endothelial progenitors, most likely because of the need to address the serious clinical sequelae associated with failure of the corneal surface that results from epithelial stem cell deficiency. A reliable means for the identification of stem cells has, therefore, become an important goal with morphological features and growth characteristics both valuable, though not definitive, indicators. A range of indicative markers for corneal epithelial stem or progenitor cells has been proposed, however, including nuclear proteins (e.g., transcription factor p63), cell membrane proteins (e.g., integrins, epidermal growth factor receptor), and cytoplasmic proteins (e.g., cytokeratins). In addition, other markers have been proposed to distinguish stem cells from differentiated cells, and these markers include various cytokeratins, intercellular adhesive proteins, and the gap junction protein connexin 43. However, no satisfactory single marker or combination of multiple molecular markers has yet been identified.

Epithelial stem cells have been found to reside within the basal epithelium at the corneal limbus [5,6], appearing smaller than adjacent basal cells [7], with a characteristic high nucleus to cytoplasmic ratio and nuclear chromatin pattern

Correspondence to: Andrew J Quantock, Structural Biophysics Research Group, Cardiff University, School of Optometry & Vision Sciences, Maindy Road, Cardiff, CF24 4HQ; Phone: +44(0)29 2087 5064; FAX: +44(0)29 2087 4859; email: QuantockAJ@cardiff.ac.uk

[8]. Although some studies [9] have suggested that stem cells seem to be present throughout the central corneal epithelium, the evidence applies to the mouse cornea only, and consensus continues to favor the corneal limbus and, in particular, deep involutions of the limbal epithelium into underlying vascularized stroma, termed the palisades of Vogt, as the major location of epithelial progenitor cells [3,5]. Basal epithelial cells at the human limbus also possess different biochemical signatures compared to epithelial cells more centrally in the cornea when examined with spectroscopic techniques [10]. In the human eye, further specialized regions have been identified within this stem cell niche, termed limbal epithelial crypts, limbal crypts, and focal stromal projections [11,12]. It seems, however, that well-defined palisades of Vogt are not present in all mammalian species; for example, palisades of Vogt are present in the pig eye [13] but reportedly absent in rabbits [14] and rodents. In the rabbit, although epithelial rete ridges projecting into the subjacent stroma, characteristic of the palisades [15], are not seen, the basement membrane zone is nonetheless undulating [16] and exhibits discontinuities of the basal lamina, reminiscent of the human limbus [14]. Chen and associates [8], in 2004, suggested that the basal invaginations of basal epithelial cells through the basement membrane at the human corneal limbus allowed close contact with the underlying vascularized stroma to facilitate nutrient transfer. More recently, Dziasko et al. [17] used a three-dimensional electron microscopy approach to demonstrate focal associations between small basal epithelial cells in crypt-rich zones of the human limbus in transplant-expired eye bank tissue and cells in the subjacent stroma. These stromal cells labeled positively for CD90 and CD105, two markers for mesenchymal stem cells, encouraging the authors to propose the limbal crypt region as a site of cellular interactions between epithelial and stromal stem cells.

Hayashi and associates [18] demonstrated N-cadherin expression by putative basal epithelial stem cells and associated melanocytes in the human limbus, implicating these cells in the modulation of the stem cell niche, and this idea has recently been expanded on by others [19]. Another concept, that specific properties of the non-epithelial stromal milieu, including the limbal microvasculature and localized connective tissue composition, may provide cues for the maintenance of a stem cell population in the limbal cornea has also been supported by several recent studies [20,21]. These putative factors have not yet been investigated in detail. Signaling pathways, including those leading to cell proliferation and differentiation, are known to be significantly modulated by some of the tissue glycosaminoglycans (GAGs), such as chondroitin sulfate (CS) and heparan sulfate (HS), bound to proteoglycans in extracellular matrices, which can function as ligands for signaling molecules. The heterogeneity of sulfation patterns on the disaccharide chains of GAGs provides the potential for the diverse reactivity of these molecules. An earlier study on articular cartilage showed that CS sulfation motifs can identify distinct cellular populations with stem cell characteristics in this tissue [22]. Here, we document the three-dimensional architecture of a putative stem cell niche in the rabbit corneal limbus with a focus on the associations between basal epithelial cells and anterior stromal cells. We also provide new information on matrix-specific CS localization subjacent to the limbal niche, using a panel of monoclonal antibodies that react with novel sulfation motif epitopes.

METHODS

Tissue acquisition: Female Japanese white rabbits (n=2; Shimizu Laboratory Supplies Co., Ltd., Kyoto) were anesthetized by intravenous administration of pentobarbital sodium solution (64.8 mg/kg, Somnopenthyl, Kyoritsu Yakuhin Corporation, Tokyo) and euthanized by scission of abdominal aorta and vena cava. Corneas were removed immediately post-mortem by an incision parallel to, and approximately 2 mm outside, the limbus. They were then cut into superior, inferior, nasal, and temporal quadrants and transferred immediately to fixatives as described below. Animals were housed and treated in accordance with the ARVO Statement for the Use of Animals in Ophthalmic and Vision Research.

A specimen of human corneal limbus was dissected from the eye of a 56-year-old male donor. The research was approved by the Human Science Ethical Committee (School of Optometry and Vision Sciences, Cardiff University, UK) and the South East Wales Research Ethics Committee (Cardiff, UK). The institutional review board granted approval with a waiver of consent as the cornea was obtained from the Bristol Corneal Transplant Service Eye Bank (Bristol Eye Hospital, UK). All tissue used in this study was obtained in accordance with the tenets of the Declaration of Helsinki, and local ethical rules were adhered to throughout. The cornea was removed to storage culture medium in the eye bank within 48 h post-mortem and obtained for study after 4 weeks when the low endothelial cell count rendered the cornea unsuitable for transplantation.

Light, transmission, and SBF SEM: Samples from each quadrant were fixed by immersion in 2.5% (v/v) glutaraldehyde and 2% (w/v) paraformaldehyde in 0.1 M sodium cacodylate buffer, pH 7.3. After storage in buffer at 4 °C, they were processed using a modification of the method described by Deerinck and Ellisman for the generation of high backscatter electron contrast for serial block face scanning electron microscopy (SBF SEM). However, the blocks

thus produced were also suitable for light microscopy on semithin (0.2–0.3 µm) sections after Toluidine blue staining and for transmission electron microscopy on unstained ultrathin (90−100 nm) sections. After the primary fixation step, full thickness, 1×5 mm tissue blocks were dissected from the limbus in each of the four corneal quadrants and transferred to 1.5% potassium ferricyanide/1% osmium tetroxide in cacodylate buffer for 1 h and then washed in distilled water. The blocks were then placed sequentially in 1% aqueous thiocarbohydrazide, 1% aqueous osmium tetroxide, and 1% aqueous uranyl acetate, each for 1 h and each followed by thorough washing in distilled water. After a further 1 h incubation in lead aspartate at 60 °C with more washes, the specimens were dehydrated in an ethanol series, from 70%, through 90% to 100%, and via propylene oxide, infiltrated, and embedded in Araldite CY212 epoxy resin over 2 days. After the resin was cured at 60 °C for 48 h, semithin sectioning was performed to identify areas of interest, and ultrathin sections cut onto uncoated G300 copper grids for examination in a JEM 1010 transmission electron microscope (Jeol (UK) Ltd, Welwyn Garden City, UK). Images of the epithelial basement membrane region, including the basal epithelium and superficial mesenchymal cells were acquired with an 11-megapixel 14-bit Orius SC1000 CCD camera (Gatan, Pleasanton, CA).

For SBF SEM, blocks containing suitably oriented regions of interest were glued to aluminum specimen pins and, after the surface was polished with ultramicrotomy, sputter-coated with gold (EM ACE 200, Leica Microsystems (UK) Ltd, Milton Keynes, UK). They were transferred to a Zeiss Sigma VP FEG SEM (Carl Zeiss Microscopy Ltd, Cambridge, UK), and sequences of up to 1,000 images acquired, with surface cuts of 50 nm, using an in-chamber Gatan 3View®2 sectioning system (Gatan UK, Oxford, UK). The image area was 10.598 × 10.598 µm, giving a resolution of 2.6 px/nm. Images were taken at 2.5 kV with 8 ms dwell time and a scan resolution of 4096 × 4096 pixels. Data sets were analyzed using Amira 5.6 software, or Image J/Fiji [23], and displayed in 3D Viewer.

Immunohistochemistry: Corneal quadrants were fixed in 4% paraformaldehyde in 0.1 M Sörensen's phosphate buffer, washed briefly, cryoprotected in a graded series of sucrose, to 30%, in buffer and frozen over dry ice in optimum cutting temperature (OCT) embedding compound for sectioning at 10 µm thickness on a cryostat at −21 °C. Sections were collected on poly-L-lysine–coated slides and washed in PBS (1X; 145 mM NaCl, 1 mM $NaH_2PO_4.2H_2O$, 18 mM $Na_2HPO_4.2H_2O$, pH 7.4) containing 0.1% Tween 20, before exposure to a panel of monoclonal antibodies, shown in Table 1, which recognize specific sulfation motifs on proteoglycans carrying chondroitin sulfate glycosaminoglycan chains. Before exposure to antibodies, all of which were diluted 1:10 in PBS/Tween, sections were blocked with PBS/Tween containing 1% bovine serum albumin (BSA) for 30 min. Antibodies were applied at 4 °C overnight. To validate the antibody reactions, some sections for each antibody were pretreated with 0.1 U/ml chondroitinase ABC (Sigma-Aldrich) in 100 mM Tris acetate buffer, pH 8.0 for 2 h at 37 °C, which degrades the CS chains carrying the epitopes they identify. Washing after antibody incubation was followed by treatment of all sections with goat anti-mouse AlexaFluor 488 secondary antibody (Molecular Probes, Invitrogen) diluted to 5 µg/ml in PBS/Tween, for 2 h, after which they were mounted under coverslips with Vectashield containing the nuclear stain 4',6-diamidino-2-phenylindole (DAPI: Vector Laboratories, Peterborough, UK). Sections obtained from the specimen of human limbus were treated in the same way as described for the rabbit tissue and exposed to 3B3, 4C3, and 6C3 primary antibodies. All sections were examined with phase and immunofluorescence microscopy with an Olympus BX40 microscope. Sections exposed to non-immune mouse serum or PBS instead of the primary antibody served as negative controls.

RESULTS

Light and transmission electron microscopy: In the Toluidine blue–stained, semithin sections obtained from all four quadrants of the rabbit limbal cornea (Figure 1), no evidence of

Table 1. Monoclonal antibodies to CS/DS proteoglycans used in this study detailing their specificity and references describing their characterization.

Antibody	Isotype	Specificity	Reference
3-B-3	IgM	native CS/DS sulphation epitopes; also, C-6-S neoepitope "stubs"after digestion with chondroitinase	[31,33]
3-C-5	IgG	native CS/DS sulphation epitopes	[22,31,35]
4-C-3	IgM	native CS/DS sulphation epitopes	[22,31,35]
6-C-3	IgM	native CS/DS sulphation epitopes	[22,31,35]
7-D-4	IgM	native CS/DS sulphation epitopes	[22,31,35]

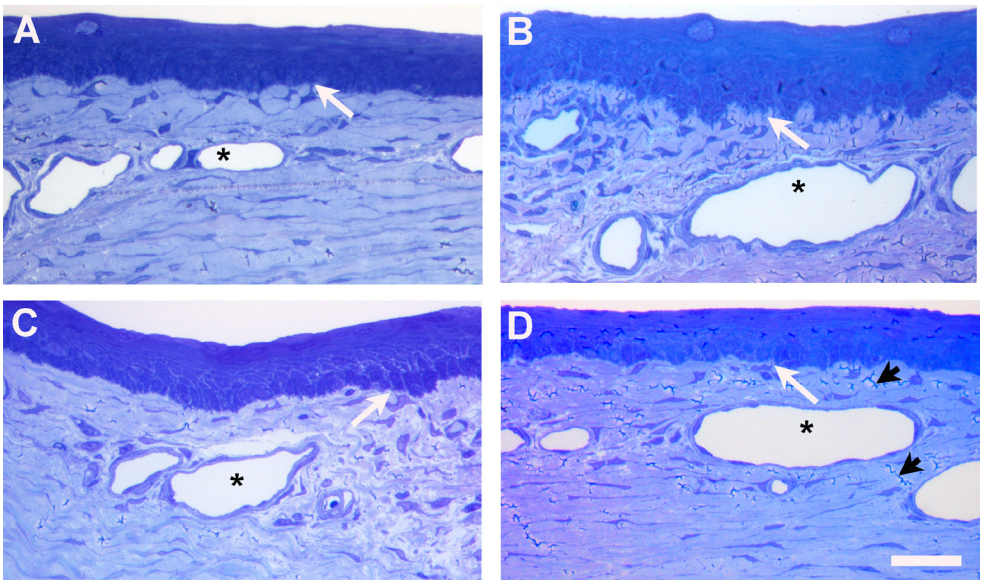

Figure 1. Toluidine blue-stained semithin sections of rabbit corneal limbus. (**A**) Superior limbal location, (**B**) Nasal, (**C**) Inferior and (**D**) Temporal. Palisades of Vogt are absent although the epithelial basement membrane has an irregular profile. Subepithelial mesenchymal cells, adjacent to capillaries (asterisks) in the superficial stroma, extend the processes distally to make contact with the basal epithelial cells (white arrows). The irregular dark lines (black arrowheads) are artifactual microfolds in the resin section, readily distinguished from the blue-stained cell processes. The central cornea is toward the right of the region illustrated in **A** and **B** and toward the left in **C** and **D**. The scale bar represents 100 µm.

structures resembling palisades of Vogt or epithelial crypts was evident. Nonetheless, the basement membrane zone in all four regions exhibited a markedly irregular profile distinct from the smooth interface present in the center of the cornea. Small blood capillaries were present in the subepithelial stroma at the limbus and in the peripheral cornea. In the former, a characteristic feature of mesenchymal cells, often in the pericapillary matrix, was the presence of cytoplasmic processes extending from the cells distally to make contact with the basement membrane and basal epithelial cells. Basal cells sometimes exhibited less basophilia than overlying layers and appeared paler-staining with Toluidine blue.

In the electron microscope, additional details of the irregular basement membrane were evident. Basal cells formed ornate lobed protrusions into the underlying stroma (Figure 2A), and their contours were followed faithfully by the basal lamina. However, at locations where it was approached by the processes emanating from mesenchymal cells the lamina often appeared discontinuous, permitting close epithelial-mesenchymal cell contact (Figure 2B). Mesenchymal cell processes at the rabbit limbus were numerous and reached extensively into the pockets created by the lobed basal membrane of the epithelial cells. Small rounded cells with a high nucleus to cytoplasm ratio were sometimes observed within the basal epithelial cell layer, invariably with multiple mesenchymal cell processes nearby (Figure 2B).

Serial block face scanning electron microscopy: Observations of epithelial cell–mesenchymal cell associations in large data sets of serial images acquired with SBF SEM of limbal corneal specimens from superior and nasal quadrants of the rabbit eye clearly showed the extent of the penetration of mesenchymal processes into the basal epithelium at numerous sites (Figure 3, and Appendix 1), with individual cells often making several connections. Three-dimensional reconstructions of selected image sequences emphasized the abundance of mesenchymal cell processes, indicating that they occasionally extended distally between adjacent basal epithelial cells (Figure 4, Appendix 2, and Appendix 3). Small capillaries were commonly identified in the superficial stroma in close proximity to sites of mesenchymal–epithelial cell interaction (Figure 5 and Appendix 4).

Immunohistochemistry: A panel of sulfation motif-specific, anti-chondroitin sulfate/dermatan sulfate (CS/DS) glycosaminoglycan antibodies provided tissue-specific staining results when applied to the rabbit corneal limbus (Figure 6). The immunoreactivity of these antibodies is indicated in Table 1. The analysis showed that some antibodies (i.e., 3B3 and 3C5; Figure 6B,E) detected no native CS/DS epitope whatsoever. However, a positive enzyme-sensitive signal was detected with antibody 7D4 in the midstroma of the peripheral cornea and was seen in association with deep capillaries in the limbus, but staining was absent from the putative stem cell zone along the limbal basement membrane (Figure 6N,O). Antibody 6C3 labeled the extracellular matrix along the basement membrane and around capillaries in the limbus at the site where epithelial–mesenchymal associations were observed with SBF SEM (Figure 6K), and staining was removed by section pretreatment with chondroitinase ABC

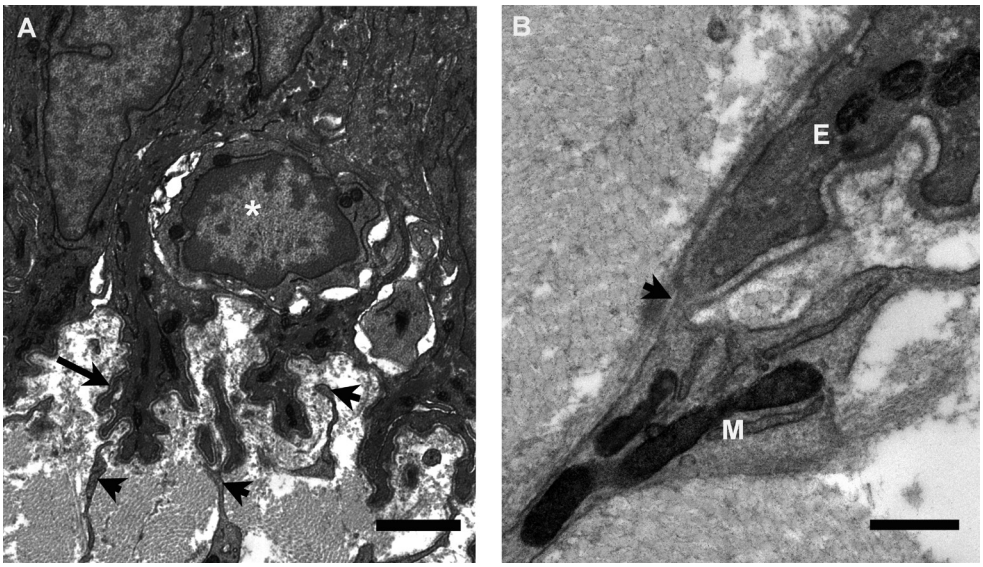

Figure 2. Transmission electron microscopy of the epithelial basement membrane zone in the rabbit corneal limbus. **A**: Basal epithelial cells surround a small rounded cell with a high nuclear to cytoplasm ratio (asterisk). Lobed processes of basal cells, with associated basal lamina (arrow), project into the superficial stroma. Numerous cytoplasmic extensions from the mesenchymal cells make contact with the basal lamina and insert between the basal cell processes (arrowheads). The scale bar represents 2 µm. **B**: Detail of the contact between the mesenchymal cell (M) and the epithelial cell process (E), where the basal lamina appears discontinuous (arrowhead). The scale bar represents 0.5 µm.

(Figure 6L). Antibody 3B3, as mentioned, detected no native epitope (Figure 6B) but showed positive localization of a CS/DS neoepitope after enzyme pretreatment (Figure 6C). Control sections were consistently negative with or without enzyme pretreatment (Figure 6Q,R). Only the 6C3 primary antibody showed positive immunofluorescence when applied to the human limbal sections (Figure 7).

DISCUSSION

Our observations of the epithelial basement membrane region in the rabbit corneal limbus confirm a lack of structures comparable to the palisades of Vogt, a characteristic feature of the human limbus, and which have previously been identified as the site of limbal epithelial progenitor or stem cells [5,24]. Nevertheless, basal epithelial cells in this region of the rabbit limbus exhibit markedly irregular profiles, sending elaborate lobed protrusions into the underlying stroma and thus present a significantly increased surface area toward the superficial mesenchyme. This observation is not new, having been identified in previous studies of the rabbit limbus [14,16]. However, our three-dimensional reconstructions of this region from serial block face scanning electron microscopy provide a new perspective and clear evidence that, in the rabbit, mesenchymal cells interact with the basal limbal epithelium just as discovered recently in the human limbus [17]. Given that the rabbit tissue examined here was processed immediately, this gives extra credence to the recently published findings of Dziasko and coworkers [17], and implies, though indirectly, of course, that gaps in the corneal basal epithelium at the limbus in human eye bank tissue are not the consequence of extended storage in preservation medium.

We suggest that lobed protrusions of basal cells in the rabbit cornea may represent the palisades in miniature, broadly fulfilling the same role. Large-volume 3D reconstructions indicate that in the rabbit, mesenchymal cells subjacent to the epithelium extend numerous cellular processes that make contact with the basal lamina and occasionally penetrate distally between basal cells making close associations. In some of these locations, the basal lamina appeared discontinuous, with the possibility that confluence may be established between the two cell types. These associations, together with the presence of small basal cells with nucleus to cytoplasmic ratios resembling cells identified as stem cells in other studies, provide strong circumstantial evidence that this site represents the stem cell niche in the rabbit corneal limbus. The presence of a source of cells in the limbus to regenerate the corneal epithelium in the rabbit has been accepted since the observation by Kinoshita et al. [25] of centripetal movement of epithelial cells from limbal origins to repair central corneal surface wounds; in addition, delayed central corneal epithelial wound healing resulted from removal of the limbal epithelium [26]. In the human eye, evidence suggested that the limbal stem cell niche is predominantly within the inferior and superior limbal quadrants, corresponding to the prominence of the palisades of Vogt, epithelial crypts, and focal stromal projections at these locations [27]. In contrast, we observed mesenchymal–epithelial associations in semithin sections from all four quadrants of the rabbit eye and

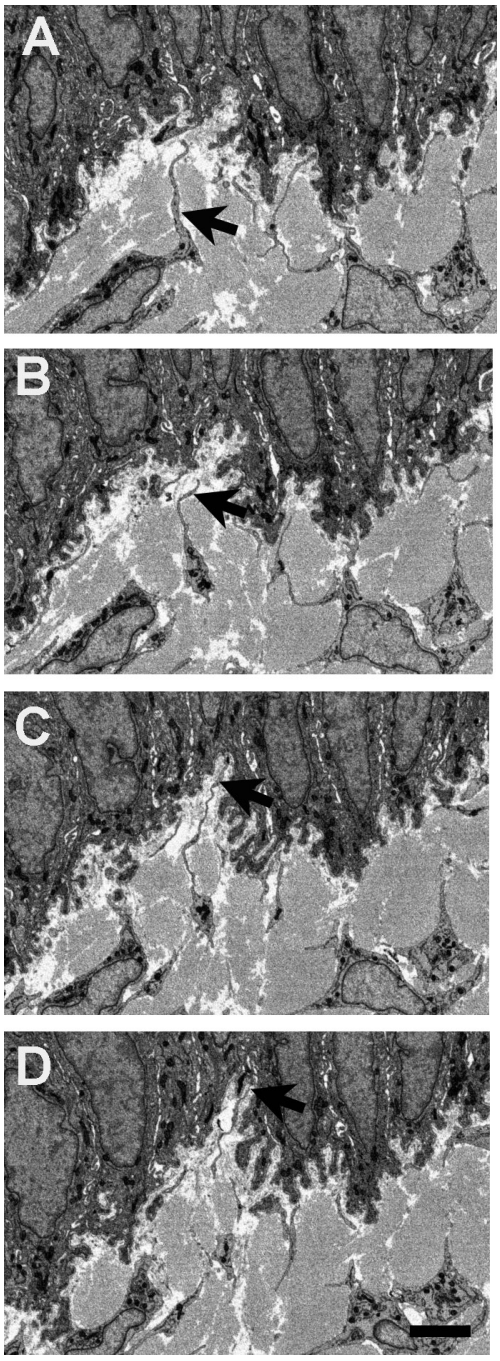

Figure 3. Reversed-contrast backscatter electron images from serial block face scanning electron microscopy of the limbal epithelial basement membrane zone in the rabbit cornea. **A**–**D** show mesenchymal–epithelial cell interactions at 20 image intervals, in approximately 1 µm increments. **A**: A subepithelial mesenchymal cell extends a process toward the basement membrane (arrow). **B**–**D**: Over the subsequent three microns, the process extends deeply into the recess formed by the lobed basal epithelial cells (arrows), appearing to make direct contact through the basal lamina (**D**). The scale bar represents 5 µm.

examined them in detail in 3D reconstructions in specimens from the superior and nasal limbus. This implies that the nature of the stem cell niche in the rabbit limbus is quite different from that in humans. Rabbit eyes exhibit some significant differences from those of humans, for example, in the blink rate (10 min versus 5–8 s between consecutive blinks in rabbit and human, respectively), anatomically in the tear film structure and stability [28], and in the presence of a nictitating membrane in rabbit. The potential influence of these factors on the distribution of limbal stem cells is unknown and requires further study.

Confirmation of stem cell potential has previously been assessed with immunocytochemical detection of specific epitopes in tissue sections [8,18], even though no definitive stem cell markers have yet been identified; cell isolation and assessment of colony-forming activity in cell culture have become another criterion employed [12,29]. An alternative approach, based on the supposition that cues for the maintenance of stem cell characteristics may reside in the extracellular matrix [20], relies upon localization of specific epitopes in the niche environment. To date, few studies have attempted to define the stem cell niche based on the matrix composition. Hayes et al. [22] used specific monoclonal antibodies (including 3B3, 4C3, 6C3, and 7D4) that recognize the sulfation patterns of the chondroitin sulfate/dermatan sulfate glycosaminoglycan chains associated with cell and extracellular matrix proteoglycans. Several of these antibodies (3B3, 4C3, and 7D4) successfully identified, with immunocytochemistry and flow cytometry, pericellular matrix and colony-forming cell populations in the superficial zone of articular cartilage from which progenitor cells had previously been isolated [30]. The remarkable heterogeneity in sulfation motifs on CS/DS proteoglycans has long been recognized as a contributory factor in which considerable diversity of structure and specificity of function could be achieved [31]. A conservative assessment indicated the human glycome may encompass around 7,000 distinct glycan determinants, including numerous CS/DS structures [32]. The precise expression of specific CS/DS motifs, together with other matrix components, could therefore define the local extracellular compartment that contributes to the maintenance of the stem cell phenotype.

The antibodies employed in our study recognize carbohydrate moieties in native (i.e., non-enzyme-predigested) chondroitin sulfate. Antibody 3B3 is believed to recognize a six-sulfated disaccharide epitope at the non-reducing terminus on CS glycosaminoglycan chains [31]. No native epitope could be detected with this antibody in the corneal limbus, but the antibody identified a neoepitope exposed with

chondroitinase pretreatment [31], which is the more conventional application of the 3B3 reagent, as it was initially raised against the enzyme-generated epitope [33]. Although the structural epitopes of antibodies 4C3, 7D4, and 6C3 remain to be precisely defined, the available evidence from chain disruption studies suggests they are all different and reside in non-terminal sequences of the CS glycosaminoglycan chain, near the linkage region to the protein core [31,34,35]. Different susceptibilities to chondroitinase digestion of these epitopes in different tissues have previously been identified, consistent with our observations of the rabbit limbus, where some residual staining persisted after enzyme treatment followed by 7D4 antibody staining, whereas all staining with antibody 6C3 was removed. Previous studies showed a diversity of staining results with native CS antibodies in cartilages from different species, as well as changes through development and in disease [31,33,34]. Interestingly, the labeling we observed in the rabbit limbus with antibodies 6C3 and 7D4 appeared somewhat similar to that reported previously in human skin with both labeling sites of vascular and neural structures: 7D4 in the deep limbal stroma and reticular dermis; 6C3 labeling the basement membrane and superficial stroma and papillary dermis, in the limbus and skin, respectively. Antibody 4C3 failed to show a significant

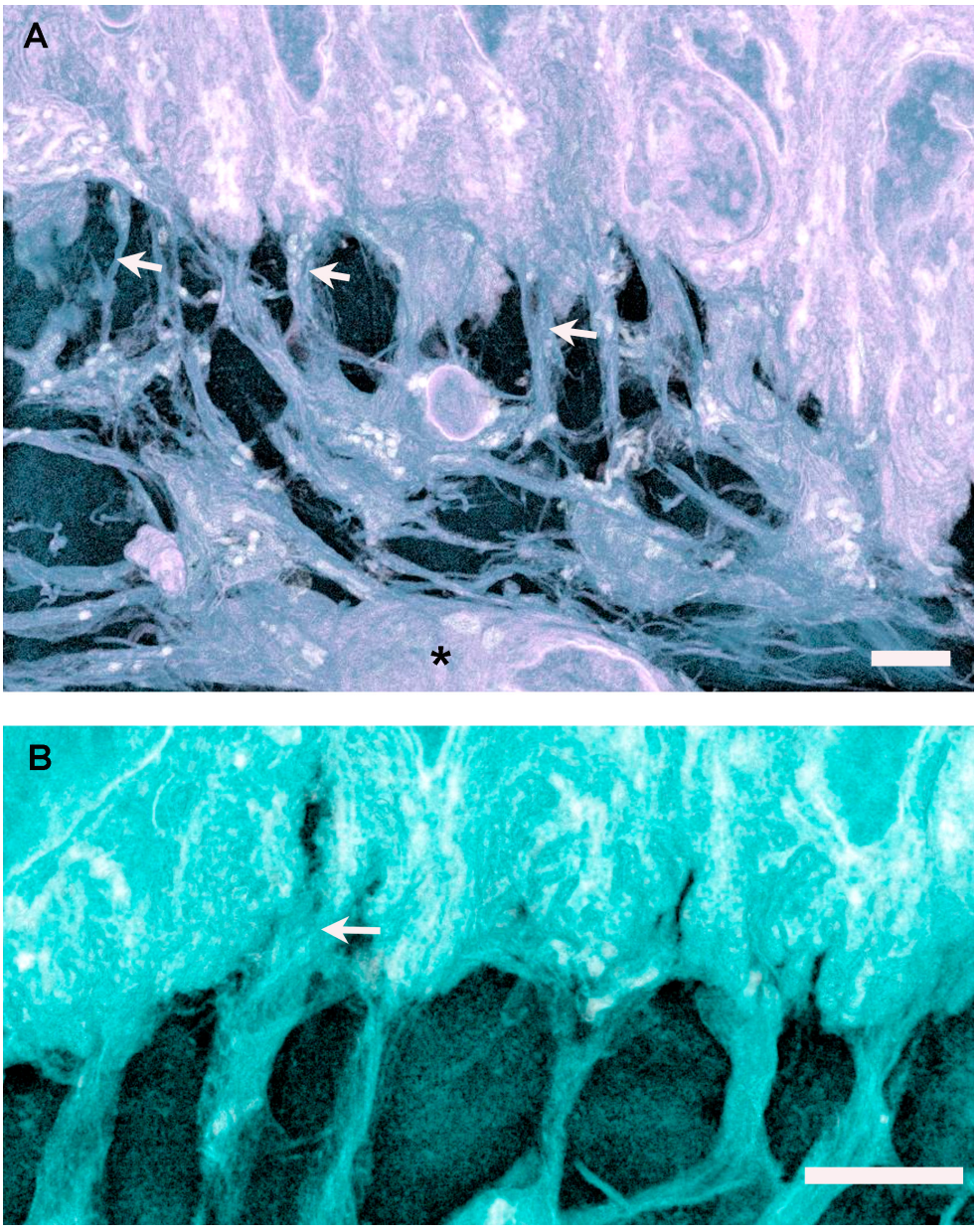

Figure 4. Three-dimensional reconstructions in ImageJ 3D Viewer of the epithelial basement membrane zone of the rabbit limbal cornea from serial block face scanning electron microscopy. **A**: A blood vessel can be seen in the superficial stroma (asterisk), below mesenchymal cells that extend numerous cytoplasmic processes (arrows) distally to contact the basal epithelial cells. The scale bar represents 4 µm. **B**: Mesenchymal cell processes form diffuse associations with epithelial cells, occasionally appearing to extend between adjacent cells (arrow). The scale bar represents 4 µm.

signal in the corneal limbus, unlike results reported in the skin. In addition, the intense labeling the antibody generated in a region of midperipheral corneal stroma was only slightly reduced by enzyme predigestion, suggesting native and neoepitope distribution for this antibody in the eye. The CS glycosaminoglycan epitope revealed by antibody 6C3 was the only component of the limbal matrix that appeared clearly coincident with the putative stem cell niche in the subepithelial stroma revealed by SBF SEM. Our preliminary results showed that antibody 6C3 also labels this site positively in the human corneal limbus.

The rabbit eye has historically proven to be a useful model for studies of corneal epithelial regeneration, and the present study indicates that in spite of morphological differences between the human and rabbit cornea at the limbus, this site has other features in common between the rabbit and human indicative of a stem cell niche at this location. The specific native CS/DS sulfation moieties, recognized by our antibodies, have been highly conserved in most animal species (chicken to human) in the stem/progenitor cell niche. We hypothesize that the collective function of CS sulfation patterns in the matrix is to act as ligands to bind and present, or sequester, a spectrum of signaling molecules, including cytokines, morphogens, chemokines and growth factors, which may lead to the initiation or inhibition of the stem to progenitor cell, to mature cell, cascades [31]. Evidence in support of this mechanism has already been reported from studies on cell migration and maturation in chondrocytes and cartilage [36,37]. Specific markers for connective tissue glycosaminoglycans can thus help define the stem cell microenvironment in the eye, although further studies are required to expand this possibility and to confirm the progenitor capability of epithelial and mesenchymal cells in the rabbit limbus.

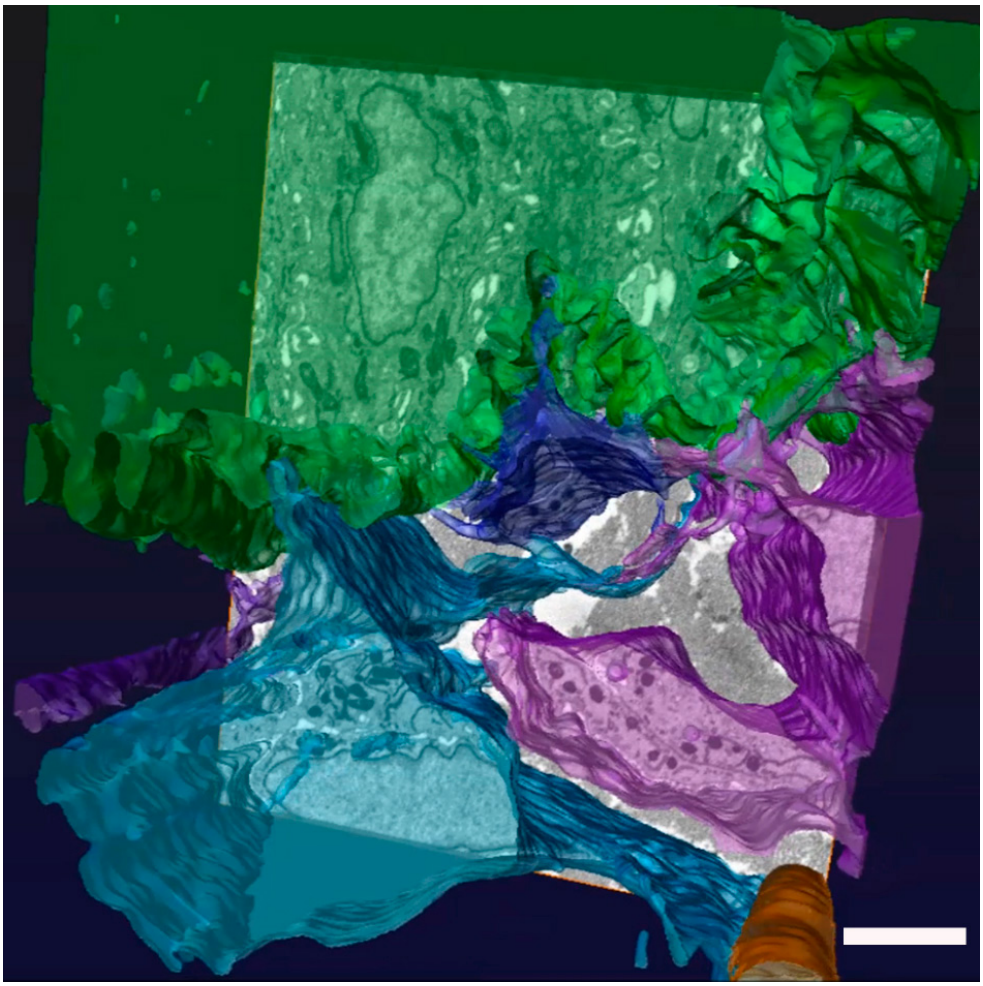

Figure 5. Three-dimensional reconstruction of the rabbit corneal limbal basement membrane zone using automated and manual segmentation techniques with Amira 5.6 software. Mesenchymal cells colored in blue and purple make associations with basal epithelial cells, in green. A superficial stromal capillary (orange) can also be seen. The scale bar represents 4 µm.

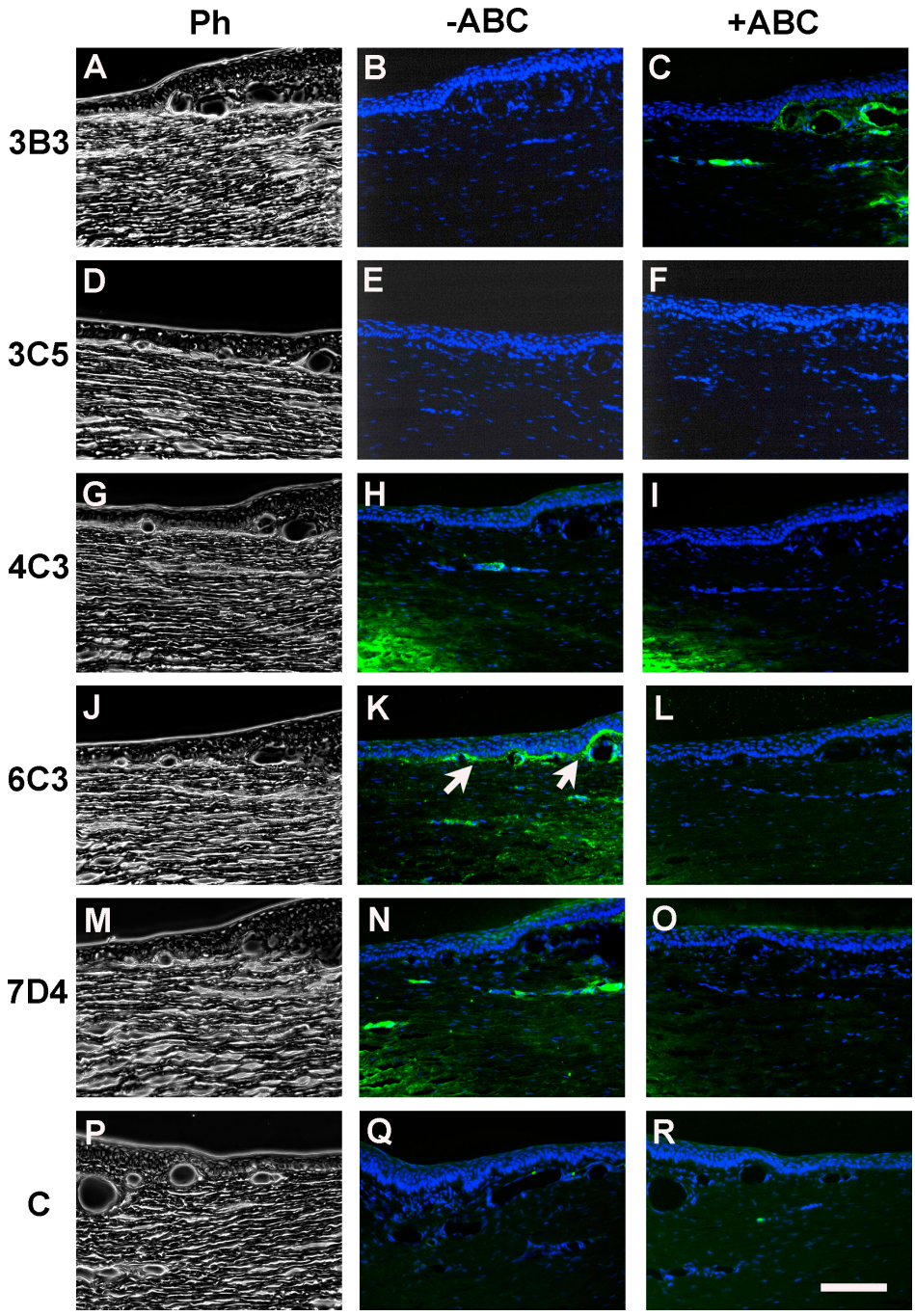

Figure 6. Immunolocalization of chondroitin sulfate proteoglycan in the rabbit corneal limbus using five sulfation motif-specific monoclonal antibodies: 3B3, 3C5, 4C3, 6C3, and 7D4. Phase contrast images are shown in the left-hand panels (**A**, **D**, **G**, **J**, **M**, and **P**); the center panels (**B**, **E**, **H**, **K**, **N**, and **Q**) show native epitope localization without section pretreatment. Antibody 6C3 labels the matrix subjacent to the limbal epithelial basement membrane (**K**, arrows). The right-hand panels (**C**, **F**, **I**, **L**, **O**, and **R**) show validation of the results by removal of native epitopes by section pretreatment with the chondroitinase ABC enzyme, and thus, the loss of the 6C3 signal (**L**). In some cases, neoepitopes are generated by enzyme treatment, as with antibody 3B3. The central cornea is toward the left in all panels, but toward the right in the controls (**P**, **Q**, and **R**). The scale bar represents 100 µm.

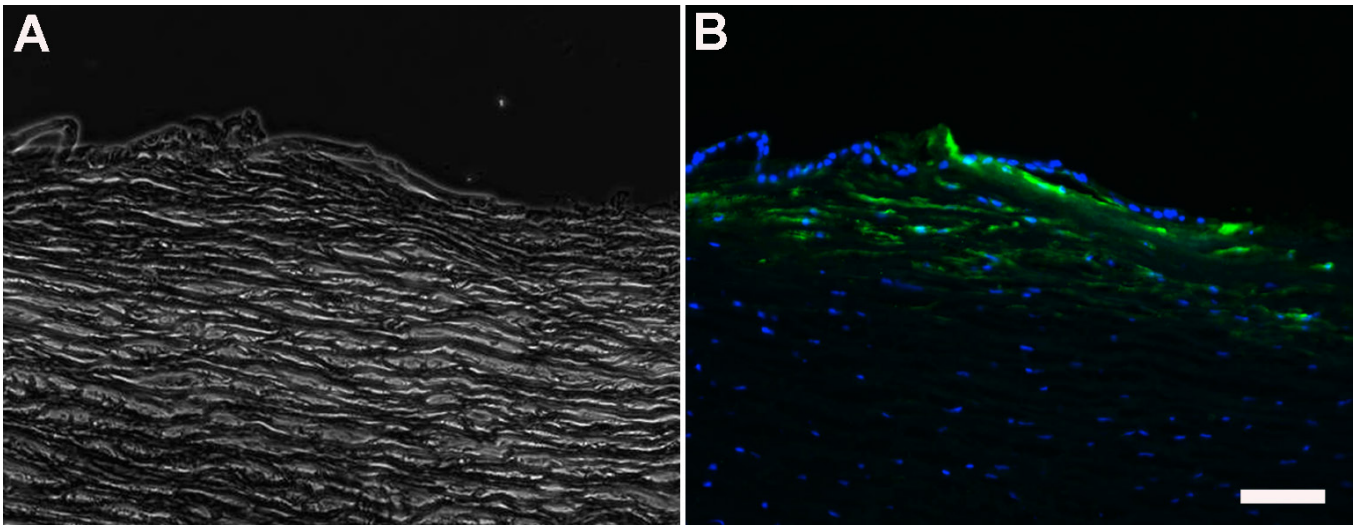

Figure 7. Light microscopy of corneal limbus from human eye. (**A**) phase microscopy image. (**B**) fluorescence microscopy image of same section. Positive immunofluorescence was detected in the sub-epithelial stroma in the region of stromal cell–epithelial cell interactions only with the CS/DS motif-specific antibody 6C3. The scale bar represents 50 µm.

APPENDIX 1: FLYTHROUGH OF 300 SERIAL IMAGES FROM SBF SEM OF RABBIT EPITHELIAL BASEMENT MEMBRANE ZONE IN CORNEAL LIMBUS.

Mesenchymal cells send processes into basal epithelium at multiple sites. To access these data, click or select the words "Appendix 1".

APPENDIX 2: VIDEO OF 3D RECONSTRUCTION MADE WITH IMAGEJ 3D VIEWER PLUGIN FROM SBF SEM IMAGES OF RABBIT LIMBAL BASEMENT MEMBRANE ZONE.

Superficial mesenchymal cells extend multiple processes to contact basal epithelial cells. To access these data, click or select the words "Appendix 2".

APPENDIX 3: VIDEO OF 3D RECONSTRUCTION MADE WITH IMAGEJ 3D VIEWER PLUGIN FROM SBF SEM IMAGES OF RABBIT LIMBAL BASEMENT MEMBRANE ZONE.

Mesenchymal cell processes extend between adjacent cells of the basal epithelial layer. To access these data, click or select the words "Appendix 3".

APPENDIX 4: VIDEO OF 3D RECONSTRUCTION MADE WITH AMIRA 5.6 SOFTWARE FROM SBF SEM IMAGES OF RABBIT LIMBAL BASEMENT MEMBRANE ZONE.

Mesencymal cells, coloured in blue and purple, associate with epithelial cells, coloured in green in the vicinity of a superficial stromal capillary, coloured in orange. To access these data, click or select the words "Appendix 4".

ACKNOWLEDGMENTS

This study was supported by a Core-to-Core Programme Award (to SK and AJQ) from the JSPS (Japan Society for the Promotion of Science), Tokyo, and Arthritis Research UK Project Grant #502413 (BC). The Zeiss Sigma VP SEM with serial block face capability was provided as part of a 5 year MRC program grant #503626 (awarded to KMM and AJQ). The authors are grateful to Prof. Vic Duance and Dr. Tony Hayes (School of Biosciences, Cardiff University) and Dr. Mayumi Ueta (Kyoto Prefectural University of Medicine, Kyoto, Japan) for invaluable contributions to this research.

REFERENCES

1. Boulton M, Albon J. Stem cells in the eye. Int J Biochem Cell Biol 2004; 36:643-57. [PMID: 15010329].
2. Schlötzer-Schrehardt U, Kruse FE. Identification and characterization of limbal stem cells. Exp Eye Res 2005; 81:247-64. [PMID: 16051216].
3. Mort RL, Douvaras P, Morley SD, Dorà N, Hill RE, Collinson JM, West JD. Stem cells and corneal maintenance – insights

from the mouse and other animal models. Results Probl Cell Differ 2012; 55:357-94. [PMID: 22918816].

4. Pinnamaneni N, Funderburgh JL. Concise Review: Stem cells in the corneal stroma. Stem Cells 2012; 30:1059-63. [PMID: 22489057].

5. Davanger M, Evensen A. Role of the pericorneal papillary structure in renewal of corneal epithelium. Nature 1971; 229:560-1. [PMID: 4925352].

6. Schermer A, Galvin S, Sun T-T. Differentiation-related expression of a major 64K corneal keratin in vivo and in culture. J Cell Biol 1986; 103:49-62. [PMID: 2424919].

7. Romano AC, Espana EM, Yoo SH, Budak MT, Wolosin JM, Tseng SCG. Different Cell Sizes in Human Limbal and Central Corneal Basal Epithelia Measured by Confocal Microscopy and Flow Cytometry. Invest Ophthalmol Vis Sci 2003; 44:5125-9. [PMID: 14638707].

8. Chen Z, de Paiva CS, Luo L, Kretzer FL, Pflugfelder SC, Li D-Q. Characterization of putative stem cell phenotype in human limbal epithelia. Stem Cells 2004; 22:355-66. [PMID: 15153612].

9. Majo F, Rochat A, Nicolas M, Jaoude GA, Barrandon Y. Oligopotent stem cells are distributed throughout the mammalian ocular surface. Nature 2008; 456:250-254. [PMID: 18830243].

10. Nakamura T, Kelly JG, Trevisan J, Cooper LJ, Bentley AJ, Carmichael PL, Scott AD, Cotte M, Susini J, Martin-Hirsch PL, Kinoshita S, Fullwood NJ, Martin FL. Microspectroscopy of spectral biomarkers associated with human corneal stem cells. Mol Vis 2010; 16:359-68. [PMID: 20520745].

11. Dua HS, Shanmuganathan VA, Powell-Richards AO, Tighe PJ, Joseph A. Limbal epithelial crypts: a novel anatomical structure and a putative limbal stem cell niche. Br J Ophthalmol 2005; 89:529-32. [PMID: 15834076].

12. Shortt AJ, Secker GA, Limb GA, Khaw PT, Daniels JT. Transplantation of ex vivo culture limbal epithelial stem cells: a review of techniques and clinical results. Surv Ophthalmol 2007; 52:483-502. [PMID: 17719371].

13. Notara M, Schrader S, Daniels JT. The porcine epithelial stem cell niche as a new model for the study of transplanted tissue-engineered human limbal epithelial cells. Tissue Eng Part A 2011; 17:741-50. [PMID: 20929285].

14. Gipson IK. The epithelial basement membrane zone of the limbus. Eye (Lond) 1989; 3:132-40. [PMID: 2515978].

15. Goldberg MF, Bron AJ. Limbal palisades of Vogt. Trans Am Ophthalmol Soc 1982; 80:155-71. [PMID: 7182957].

16. Góes RM, Barbosa FL, De Faria-e-Sousa, SJ, Haddad A. Morphological and autoradiographic studies on the corneal and limbal epithelium of rabbits. Anat Rec 2008; 291:191-203. .

17. Dziasko MA, Armer HE, Levis HJ, Shortt AJ, Tuft S, Damiels JT. Localisation of epithelial cells capable of holoclone formation *in vitro* and direct interaction with stromal cells in the native human limbal crypt. PLoS ONE 2014; 9:e94283- [PMID: 24714106].

18. Hayashi R, Yamato M, Sugiyama H, Sumide T, Yang J, Okano T, Tano Y, Nishida K. N-cadherin is expressed by putative stem-progenitor cells and melanocytes in the human limbal epithelial stem cell niche. Stem Cells 2007; 25:289-96. [PMID: 17008425].

19. Dziasko MA, Tuft SJ, Daniels JT. Limbal melanocytes support limbal epithelial stem cells in 2D and 3D microenvironments. Exp Eye Res 2015; 138:70-9. [PMID: 26142953].

20. Espana EM, Kawakita T, Romano A, Di Pascuale M, Smiddy R, Liu C-Y, Tseng SCG. Stromal niche controls the plasticity of limbal and corneal epithelial differentiation in a rabbit model of recombined tissue. Invest Ophthalmol Vis Sci 2003; 44:5130-5. [PMID: 14638708].

21. Huang M, Wang B, Wan P, Liang X, Wang X, Liu Y, Zhou Q, Wang Z. Roles of limbal microvascular net and limbal stroma in regulating maintenance of limbal epithelial stem cells. Cell Tissue Res 2015; 359:547-63. [PMID: 25398719].

22. Hayes AJ, Tudor D, Nowell MA, Caterson B, Hughes CE. Chondroitin sulphate sulfation motifs as putative biomarkers for isolation of articular cartilage progenitor cells. J Histochem Cytochem 2008; 56:125-38. [PMID: 17938280].

23. Abramoff MD, Magelhaes PJ, Ram SJ. Image Processing with ImageJ. Biophotonics International 2004; 11:36-42. .

24. Townsend WM. The limbal palisades of Vogt. Trans Am Ophthalmol Soc 1991; 89:721-56. [PMID: 1808821].

25. Kinoshita S, Friend J, Toft RA. Sex chromatin of donor corneal epithelium in rabbits. Invest Ophthalmol Vis Sci 1981; 21:434-41. [PMID: 7024181].

26. Huang AJW, Tseng SCG. Corneal epithelial wound healing in the absence of limbal epithelium. Invest Ophthalmol Vis Sci 1991; 32:96-105. [PMID: 1702774].

27. Shortt AJ, Secker GA, Munro PM, Khaw PT, Daniels JT. Characterization of the limbal epithelial stem cell niche: novel imaging techniques permit in vivo observation and targeted biopsy of limbal epithelial stem cells. Stem Cells 2007; 25:1402-9. [PMID: 17332511].

28. Wei XE, Markoulli M, Zhao Z, Willcox MDP. Tear film break-up time in rabbits. Clin Exp Optom 2013; 96:70-5. [PMID: 22971008].

29. Pellegrini G, Golisano O, Paterna P, Lambiase A, Bonini S, Rama P, De Luca M. Location and clonal analysis of stem cells and their differential progeny in the human ocular surface. J Cell Biol 1999; 145:769-82. [PMID: 10330405].

30. Dowthwaite GP, Bishop JC, Redman SN, Khan IM, Rooney P, Evans DJ, Haughton L, Bayram Z, Boyer S, Thonson B, Wolfe MS, Archer CW. The surface of articular cartilage contains a progenitor cell population. J Cell Sci 2004; 117:889-97. [PMID: 14762107].

31. Caterson B. Fell-Muir Lecture:Chondroitin sulphate glycosaminoglycans: fun for some and confusion for others. Int J Exp Pathol 2012; 93:1-10. [PMID: 22264297].

32. Cummings RD. The repertoire of glycan determinants in the human glycome. Mol Biosyst 2009; 5:1087-104. [PMID: 19756298].

33. Caterson B, Christner JE, Baker JR, Couchman JR. Production and characterization of monoclonal antibodies directed against connective tissue proteoglycans. Fed Proc 1985; 44:386-93. [PMID: 2578417].

34. Caterson B, Mahmoodian F, Sorrell JM, Hardingham TE, Bayliss MT, Carney SL, Ratcliffe A, Muir H. Modulation of native chondroitin sulphate structure in tissue development and in disease. J Cell Sci 1990; 97:411-7. [PMID: 1705939].

35. Sorrell JM, Mahmoodian F, Schafer IA, Davis B, Caterson B. Identification of monoclonal antibodies that recognize novel epitopes in native chondroitin/dermatan sulfate glycosaminoglycan chains: their use in mapping functionally distinct domains of human skin. J Histochem Cytochem 1990; 38:393-402. [PMID: 1689338].

36. Davies LC, Blain E, Caterson B, Duance VC. Chondroitin sulphate impedes the migration of a sub-population of articular cartilage chondrocytes. Osteoarthritis Cartilage 2008; 16:855-64. [PMID: 18222711].

37. Davies LC, Blain EJ, Gilbert SJ, Caterson B, Duance VC. The potential of IGF-1 and TGF-1 for promoting ‘‘adult’’ articular cartilage repair: an in vitro study. Tissue Eng 2008; 14:1251-61. .

Articles are provided courtesy of Emory University and the Zhongshan Ophthalmic Center, Sun Yat-sen University, P.R. China. The print version of this article was created on 29 December 2015. This reflects all typographical corrections and errata to the article through that date. Details of any changes may be found in the online version of the article.